Available online at www.sciencedirect.com
SCIENCE DIRECT®
Journal of Sound and Vibration 264 (2003) 1057–1072
JOURNAL OF SOUND AND VIBRATION
www.elsevier.com/locate/jsvi

Reference motion in deformable bodies under rigid body motion and vibration. Part II: evaluation of the coefficient of restitution for impacts

J.L. Escalona*, J. Valverde, J. Mayo, J. Domínguez

Department of Mechanical Engineering, University of Seville, Camino de los Descubrimientos s/n, 41092 Seville, Spain

Received 22 February 2002; accepted 29 March 2002

Abstract

The dynamic analysis of rigid body impacts is usually performed by using the coefficient of restitution as a measure of the mechanical energy lost in the process. The coefficient of restitution provides an algebraic equation that allows impulse–momentum balance equations to be solved. This paper reports a method for calculating the kinematic coefficient of restitution for the impact of deformable bodies by using a numerical simulation procedure. Calculations were done within the framework of the *floating reference frame approach*. As shown here for the first time, discriminating between *reference velocities* and *rigid body equivalent velocities* is essential with a view to accurately calculating the kinematic coefficient of restitution. Thus, the velocities at which the contact points approach and depart must be calculated as rigid body equivalent velocities. If references velocities are used instead, the resulting coefficient of restitution lacks physical significance. The proposed method is illustrated with two applications, namely: an axial impact of a rigid body on a deformable rod and a transverse impact of a beam on a fixed stop.

1. Introduction

Impulse dynamics assumes that collisions between rigid bodies are instantaneous. This hypothesis is not only an approximation to physical evidence but also a pre-requisite for the dynamic treatment of the impact. The contact process during the impact of two bodies is usually inappreciable to the observer. In fact, the contact time is much shorter than the characteristic evolution time of rigid body motions. However, even if the contact process were to be analyzed in

*Corresponding author.
E-mail address: escalona@us.es (J.L. Escalona).

0022-460X/03/$ - see front matter © 2002 Elsevier Science Ltd. All rights reserved.
doi:10.1016/S0022-460X(02)01188-4

a continuous manner, this would be impossible if the bodies were assumed to be rigid. In fact, in order to be able to perform a continuous analysis of the impact, the contact points must acquire the same normal velocity instantaneously at the first instant of the collision. This requires a finite jump in the velocities of the bodies, which would result in the inertial and contact forces being infinite at contact time. Consequently, one has to resort to impulse dynamics and cannot calculate the contact forces if the bodies are assumed to be rigid. If contact is assumed to occur over an infinitesimal interval—so the co-ordinates defining the position of the bodies will not change—one can integrate the equations of motion over such an interval. This yields a system of algebraic equations the unknowns of which are the velocities of the bodies upon colliding and the impulse of the contact force—plus that of reactive forces, if any. However, this equation system is indeterminate and rendering it determinate entails including an additional equation to introduce the restitution condition. The restitution condition expresses the ratio between the velocities at which the contact points approach and depart. Such a ratio is known as the "kinematic coefficient of restitution" [1]. The coefficient of restitution is a number ranging from zero to one. It can never be less than zero as the bodies would otherwise interpenetrate each other upon contact. Also, it cannot be greater than unity as this would reflect an increase in the mechanical energy of the bodies by effect of the impact. The amount of mechanical energy lost in the impact increases with decrease in the coefficient of restitution.

The coefficient of restitution thus depends both on the local geometry—around the contact zone—and the overall geometry of the bodies, as well as on the constants that dictate their behavior during the deformation (viz. elastic, elastoplastic, viscoelastic coefficients) and the relative impact velocity [2]. Traditionally, the coefficient of restitution has been determined experimentally. However, the range of possible situations is so wide and measurements are so costly that, in practice, the data required to calculate it are rarely accessible. Currently available methods for the dynamic analysis of deformable bodies allow the coefficient of restitution to be calculated by numerical simulation. This paper reports a formula for evaluating the kinematic coefficient of restitution.

The amount of mechanical energy lost on impact at a moderate velocity (i.e., when the bodies remain intact upon colliding), which is estimated through the coefficient of restitution, arises mainly from plasticity and friction in the contact zone, as well as from internal vibrations in the bodies (elastic wave propagation). When the impact involves bodies with a massive geometry (e.g., spheres), local energy losses are much more substantial than losses due to internal vibration; the opposite is true of slender bodies (e.g., beams, plates and shells). In order to analyze the vibrations produced by the impact, the bodies must be modelled as if they were flexible, even though they can reasonably be modelled as rigid bodies under the usual operating conditions. It should be noted that the internal vibration energy is lost mechanical energy when the bodies are modelled as rigid but not when modelled as flexible.

The coefficient of restitution calculated in this work affords the dynamic analysis of bodies that can normally be assumed to be rigid. As noted earlier, this hypothesis does not hold in the presence of collisions, which entail analyzing the impact in a continuous manner. For this reason, the bodies examined here were modelled as deformable bodies for the dynamic analysis of impacts in order to concentrate the studied process on a single coefficient. This is the coefficient to be used in the restitution condition when the impact is analyzed on the assumption of rigid bodies.

The dynamic analysis of impacts between rigid bodies can be performed by using continuous-contact force–indentation models [3–7], the constraint addition–deletion technique [8–10] and the generalized impulse–momentum balance equations [11–14].

Continuous contact force–indentation models rely on the assumption that the colliding body volumes can interpenetrate during the process and calculate the contact force as a function of indentation and the indentation velocity (using, for example, the Hertz force–indentation static relation). This technique can be used on the assumption that the bodies are rigid except in the region around the contact surfaces (massive geometry bodies) or that the bodies are also flexible on the whole (slender bodies).

The constraint addition–deletion method [8–10] involves keeping the contact points together during impact by applying kinematic constraints. The contact force is obtained as the reaction force associated to the constraint. The constraint is eliminated from the system of motion equations—and the impact process is thus terminated—when the reaction force becomes a traction force. The most serious problem of this technique is posed by the calculation of the velocity shared by both contact points early during the impact.

Generalized conservation equations [11–14] constitute an extension of impulse dynamics to flexible bodies. When applied to bodies assumed to be elastic, the algebraic equations of balance must be solved not one, but several times before the analysis of the impact is finished [13]. The number of balances to be performed increases with increasing number of degrees of freedom used to model the deformable body. As a result, the solutions are subject to convergence problems when the number of elastic co-ordinates in the deformable model is changed. The restitution condition must thus be revised to avoid convergence problems.

This paper is structured as follows: the following section derives the impulse–momentum balance equations for the impact of rigid bodies in planar motion. The equation that represents the restitution condition includes the coefficient that is calculated in the subsequent sections. Section 3 describes the simulation technique used to analyze the impact of slender deformable bodies. Section 4 provides a formula for calculating the kinematic coefficient of restitution that includes the rigid body equivalent velocities as defined in Ref. [15]. Section 5 describes the dynamic simulation of the two examples used to illustrate the impact of rigid bodies on flexible bodies (viz. an axial impact on a rod and a transverse impact of an elastic beam). These two examples use different reference conditions and shape functions to describe deformation in the bodies. The coefficients of restitution thus calculated under the different conditions are consistent. Finally, Section 6 summarizes the results and draws several conclusions from them.

2. Balance equations for rigid body impacts

The impulse-momentum balance equations used apply to two free bodies with planar motion (see Fig. 1). The position and orientation of the bodies, i and j, are described in terms of the position of the origin of the reference systems bound to each body at its centre of gravity, $\mathbf{R}^i$ and $\mathbf{R}^j$, and their orientation with respect to a global reference system, θ^i and θ^j. The position of the contact point, C, with respect to the local reference systems is given by $\mathbf{r}^i_C$ and $\mathbf{r}^j_C$. The unit vector $\mathbf{n}$ defines the direction of the normal shared by the body surfaces at the contact point; it was assumed to point at the inside of body j. Vector $\mathbf{n}$ defines the direction where the normal contact

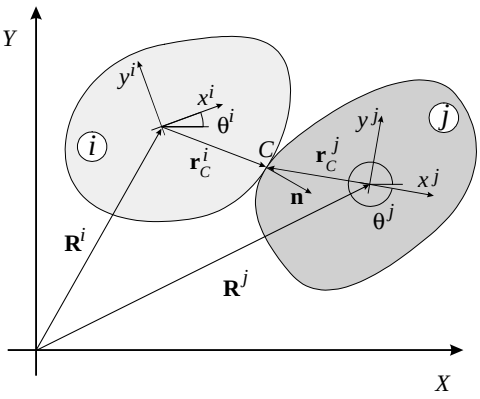

Fig. 1. Impact of freely moving bodies.

force acts. Friction between the bodies was assumed not to exist—and the transverse contact force to be zero as a result. The equations of motion for the bodies during impact were as follows:

$$\mathbf{M}\ddot{\mathbf{q}} = \mathbf{Q}_{Fc} + \mathbf{Q}_{ext}, \tag{1}$$

$$\mathbf{M} = \mathrm{diag}\begin{bmatrix} m^i & m^i & I^i & m^j & m^j & I^j \end{bmatrix}, \tag{2}$$

$$\mathbf{q} = \begin{bmatrix} X^i & Y^i & \theta^i & X^j & Y^j & \theta^j \end{bmatrix}, \tag{3}$$

where X^i, Y^i, X^j and Y^j are the components of $\mathbf{R}^i$ and $\mathbf{R}^j$, respectively, $\mathbf{Q}_{Fc}$ is the generalized vector of the contact force and $\mathbf{Q}_{ext}$ the generalized vector of other external forces acting on the bodies. Vector $\mathbf{Q}_{Fc}$ can be expressed in matrix form as

$$\mathbf{Q}_{Fc} = \mathbf{B}^{\mathrm{T}}\mathbf{n}F_c, \tag{4}$$

where F_c is the contact force and $\mathbf{B}$ a geometric matrix called the "incidence matrix" [14] that is defined as

$$\mathbf{B} = \begin{bmatrix} -1 & 0 & Y_P^i & 1 & 0 & -Y_P^j \\ 0 & -1 & -X_P^i & 0 & 1 & X_P^j \end{bmatrix}, \tag{5}$$

where X_P^i, Y_P^i, X_P^j and Y_P^j are the global components of $\mathbf{r}_C^i$ and $\mathbf{r}_C^j$, respectively. Integration of the equations of motion over the contact interval, $[0, t_c]$, which is assumed to be infinitesimal, yields

$$\lim_{t_c \to 0} \int_0^{t_c} \mathbf{M}\ddot{\mathbf{q}}\,\mathrm{d}t = \lim_{t_c \to 0} \int_0^{t_c} \left(\mathbf{B}^{\mathrm{T}}\mathbf{n}F_c + \mathbf{Q}_{ext}\right)\mathrm{d}t \quad \Rightarrow \quad \mathbf{M}\Delta\dot{\mathbf{q}} = \mathbf{B}^{\mathrm{T}}\mathbf{n}I \tag{6}$$

being $\Delta\mathbf{q}$ the velocity jump undergone by the co-ordinates of the system and I the impulse of the contact force. In the previous integration, a zero impulse for all other forces on the body was assumed. Other external forces are assumed to be much smaller than the contact force and their impulse to be negligible as a result. The six algebraic expressions contained in Eq. (6) are generalized impulse–momentum balance equations. They contain seven unknowns, viz. the six components of $\Delta\mathbf{q}$ and the impulse I. The additional equation required to render the system determinate is that of the restitution condition, based on which the relationship between the normal departure velocity at the contact points and the normal approach velocity is known. Such

a relationship is given by the coefficient of restitution, e:

$$e = -\frac{\mathbf{n}^{\mathrm{T}}\left(\dot{\mathbf{R}}_C^j - \dot{\mathbf{R}}_C^i\right)^+}{\mathbf{n}^{\mathrm{T}}\left(\dot{\mathbf{R}}_C^j - \dot{\mathbf{R}}_C^i\right)^-}, \tag{7}$$

where superscripts "−"and "+" denote the values immediately preceding ($t=0$) and following ($t=t_c$) impact. The restitution condition can also be expressed in matrix form

$$e = -\frac{\mathbf{n}^{\mathrm{T}}\mathbf{B}\dot{\mathbf{q}}^+}{\mathbf{n}^{\mathrm{T}}\mathbf{B}\dot{\mathbf{q}}^-} \;\Rightarrow\; \mathbf{n}^{\mathrm{T}}\mathbf{B}\dot{\mathbf{q}}^+ = -e\mathbf{n}^{\mathrm{T}}\mathbf{B}\dot{\mathbf{q}}^-. \tag{8}$$

Subtracting vector $\mathbf{n}^{\mathrm{T}}\mathbf{B}\dot{\mathbf{q}}^-$ from both sides of the previous equation yields

$$\mathbf{n}^{\mathrm{T}}\mathbf{B}\Delta\dot{\mathbf{q}} = -(1+e)\mathbf{n}^{\mathrm{T}}\mathbf{B}\dot{\mathbf{q}}^- \tag{9}$$

Eq. (9), together with the six expressions of Eq. (6) constitute a determinate system of linear algebraic equations that can also be expressed in matrix form

$$\begin{bmatrix} \mathbf{M} & -\mathbf{B}^{\mathrm{T}}\mathbf{n} \\ -\mathbf{n}^{\mathrm{T}}\mathbf{B} & 0 \end{bmatrix} \begin{bmatrix} \Delta\dot{\mathbf{q}} \\ I \end{bmatrix} = \begin{bmatrix} \mathbf{0} \\ -(1+e)\mathbf{n}^{\mathrm{T}}\mathbf{B}\dot{\mathbf{q}}^- \end{bmatrix}. \tag{10}$$

An explicit solution to this equation system can be obtained as follows: vector $\Delta\dot{\mathbf{q}}$ can be expressed as a function of the impulse, I, by solving Eq. (6) for it

$$\Delta\dot{\mathbf{q}} = \mathbf{M}^{-1}\mathbf{B}^{\mathrm{T}}\mathbf{n}I \tag{11}$$

Substituting this equation into Eq. (9) yields

$$\mathbf{n}^{\mathrm{T}}\mathbf{B}\mathbf{M}^{-1}\mathbf{B}^{\mathrm{T}}\mathbf{n}I = -(1+e)\mathbf{n}^{\mathrm{T}}\mathbf{B}\dot{\mathbf{q}}^- \;\Rightarrow\; I = -(1+e)\hat{m}\mathbf{n}^{\mathrm{T}}\mathbf{B}\dot{\mathbf{q}}^- \tag{12}$$

where the scalar quantity $\hat{m}$, which possesses mass dimensions, is given by

$$\hat{m} = \left[\mathbf{n}^{\mathrm{T}}\mathbf{B}\mathbf{M}^{-1}\mathbf{B}^{\mathrm{T}}\mathbf{n}\right]^{-1} \tag{13}$$

Substituting Eq. (12) into Eq. (11) yields

$$\Delta\dot{\mathbf{q}} = -[(1+e)\hat{m}]\mathbf{M}^{-1}\mathbf{B}^{\mathrm{T}}\mathbf{n}\mathbf{n}^{\mathrm{T}}\mathbf{B}\dot{\mathbf{q}}^- = -[(1+e)\hat{m}]\mathbf{D}\dot{\mathbf{q}}^- \tag{14}$$

where $\mathbf{D} = \mathbf{M}^{-1}\mathbf{B}^{\mathrm{T}}\mathbf{n}\mathbf{n}^{\mathrm{T}}\mathbf{B}$. Eq. (14) determines the velocity jump as a function of the coefficient of restitution and the velocities of the bodies immediately before impact.

The fact that the coefficient of restitution can never be less than zero has physical significance; otherwise, the rigid volumes would interpenetrate each other upon colliding. Its upper bound, unity, arises from the fact that greater values would increase the kinetic energy of the system upon contact of the bodies. The proof is well known but not easily accessible in the literature, so it is described below. The loss of kinetic energy due to collision can be expressed as

$$\begin{aligned} \Delta T = T^- - T^+ &= \tfrac{1}{2}\left(\dot{\mathbf{q}}^{-\mathrm{T}}\mathbf{M}\dot{\mathbf{q}}^- - (\dot{\mathbf{q}}^- + \Delta\dot{\mathbf{q}})^{\mathrm{T}}\mathbf{M}(\dot{\mathbf{q}}^- + \Delta\dot{\mathbf{q}})\right) \\ &= \tfrac{1}{2}\left(-2\dot{\mathbf{q}}^{-\mathrm{T}}\mathbf{M}\Delta\dot{\mathbf{q}} - \Delta\dot{\mathbf{q}}^{\mathrm{T}}\mathbf{M}\Delta\dot{\mathbf{q}}\right) \end{aligned} \tag{15}$$

Substituting Eq. (14) into Eq. (15) yields

$$\Delta T = T^- - T^+ = \tfrac{1}{2}\left(2(1+e)\hat{m}\dot{\mathbf{q}}^{-\mathrm{T}}\mathbf{M}\mathbf{D}\dot{\mathbf{q}}^- - (1+e)^2\hat{m}^2\dot{\mathbf{q}}^{-\mathrm{T}}\mathbf{D}^{\mathrm{T}}\mathbf{M}\mathbf{D}\dot{\mathbf{q}}^-\right) \tag{16}$$

The following identities are immediately apparent:

$$\begin{aligned} \hat{m}\mathbf{D}^{\mathrm{T}}\mathbf{M}\mathbf{D} &= \mathbf{H}, \\ \mathbf{M}\mathbf{D} &= \mathbf{H}, \end{aligned} \tag{17}$$

where $\mathbf{H}$ is a geometric matrix defined as

$$\mathbf{H} = \mathbf{B}^{\mathrm{T}}\mathbf{n}\mathbf{n}^{\mathrm{T}}\mathbf{B} \tag{18}$$

Substitution of the identities in Eq. (17) into Eq. (16) yields

$$\Delta T = T^{-} - T^{+} = \tfrac{1}{2}\left(1 - e^2\right)\hat{m}\dot{\mathbf{q}}^{-\mathrm{T}}\mathbf{H}\dot{\mathbf{q}}^{-}. \tag{19}$$

Eq. (19) shows that the loss of kinetic energy is proportional to $(1–e^2)$, zero at $e=1$ and highest at $e=0$.

3. Dynamic analysis of impacts on flexible bodies

This section describes the procedure used for the dynamic analysis of impacts on flexible beams. Deformations in the bodies were determined by using the Rayleigh–Ritz method as described in Ref. [15]. The shape functions thus obtained, however, could not accurately describe the local deformations produced by the impact. Such functions are only appropriate for representing structural—not local—deformations. For this reason, although the impact was analyzed in a continuous manner and the bodies deformed during the process, their volumes were allowed to interpenetrate during collision. Based on body indentation, γ, the contact force was calculated in a continuous manner. The value thus obtained was included in the equations of motion as a generalized force that will generally possess some component in the elastic and reference co-ordinates. Fig. 2 shows an instant of the impact between two slender bodies and the indentation undergone by both of them. Bodies are shown in the undeformed and deformed configurations. The position vectors of the contact points (which do not coincide for both bodies) with respect to the body frames of reference are represented as the addition of the position vectors in the undeformed conurations plus the elastic displacement vectors.

The Hertz elastic force–indentation relation is used to calculate the contact force. Such a relation is applicable to bodies with a non-conformant soft geometry around the contact zone. The contact force was thus calculated from

$$\begin{aligned} F_c &= K_h\gamma^{3/2}, \\ \gamma &= \gamma\left(\mathbf{q}_r, \mathbf{q}_f\right), \end{aligned} \tag{20}$$

where K_h is a constant [16] that depends on the elastic properties of the bodies, Young's modulus and the Poisson coefficient, as well as on the local curvature of the bodies in contact. Indentation, γ, is calculated geometrically as a function of the system co-ordinates.

It should be noted that the Hertz force–indentation relation is elastic, so this model cannot be used to describe local energy losses (plasticity). This effect can be represented by using an elastoplastic force–indentation relation [6,7]. Therefore, the coefficient of restitution calculated using the proposed method considered the portion of kinetic energy prior to the impact that became vibrational energy in the bodies (kinetic vibrational energy plus deformation energy) upon colliding. However, simply replacing the Hertz relation with an elastoplastic one allowed the energy lost as local plasticity to be calculated.

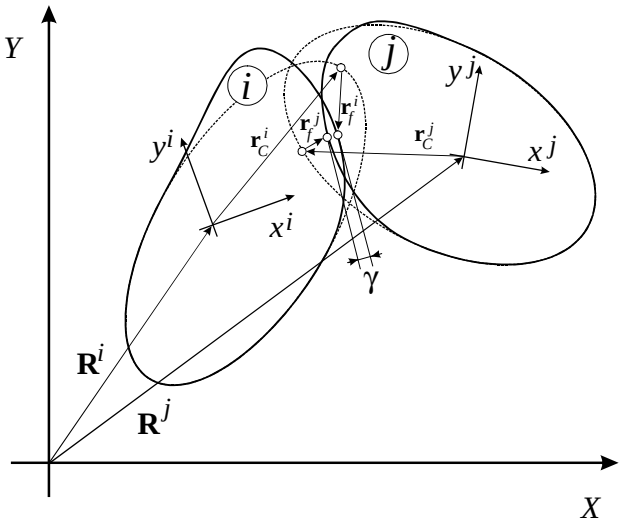

Fig. 2. Impact of slender bodies.

4. Evaluation of the dynamic coefficient of restitution

The coefficient of restitution to be evaluated using the proposed model was that to be included in the algebraic equation system (10) if the bodies were assumed to be rigid. As noted in Ref. [15], the reference velocities do not represent rigid body velocities. Consequently, calculating the kinematic coefficient of restitution entailed evaluating the relationship between the approach and departure velocities of the contact points in terms of the rigid body equivalent velocities. These angular and translation velocities were defined in Ref. [15]. The kinematic coefficient of restitution was obtained from the following expression:

$$e = -\frac{\mathbf{n}^{\mathrm{T}}\left[(\mathbf{V}_{RB})^j_C - (\mathbf{V}_{RB})^i_C\right]^+}{\mathbf{n}^{\mathrm{T}}\left[(\mathbf{V}_{RB})^j_C - (\mathbf{V}_{RB})^i_C\right]^-} = -\frac{\mathbf{n}^{\mathrm{T}}\left[\mathbf{V}^j_{RB} + \omega^j_{RB}\mathbf{A}^j_\theta \bar{\mathbf{r}}^j_C - \left(\mathbf{V}^i_{RB} + \omega^i_{RB}\mathbf{A}^i_\theta \bar{\mathbf{r}}^i_C\right)\right]^+}{\mathbf{n}^{\mathrm{T}}\left[\mathbf{V}^j_{RB} + \omega^j_{RB}\mathbf{A}^j_\theta \bar{\mathbf{r}}^j_C - \left(\mathbf{V}^i_{RB} + \omega^i_{RB}\mathbf{A}^i_\theta \bar{\mathbf{r}}^i_C\right)\right]^-}. \tag{21}$$

It should be noted that the velocities at the contact points used did not match the actual velocities in the description of floating reference systems, but other, fictitious velocities that such points would have if the bodies were assumed to be rigid.

5. Examples

5.1. Axial impact of a rigid body on a flexible rod

This section examines the axial impact of a rigid body on a flexible rod (see Fig. 3). This is a well-known case of impact-induced vibrations [2,17]. The contact process generates a compression

wave that travels along the elastic rod, compressing sections and propelling them as it moves. When the wave reaches the free end, it is reflected in such a way that it pulls the cross sections as it goes. The process would repeat itself indefinitely if no dampening existed. Those sections not being crossed by the elastic wave at a given time remain quiescent, with no velocity or stress. Because the wave propagates very rapidly, the observer may perceive that the rod moves with a constant velocity. In fact, the rod sections alternate between motion and rests, and progress in steps. This process is illustrated in Fig. 4, where the arrows outside the wave pulses indicate their propagation velocity, those inside them the stress of the sections (compression those that point inwards and tensile those that point outwards) and their material velocity.

This problem was analyzed using two types of reference conditions and shape functions. In both cases, the undeformed position of the origin of the local reference system associated to rigid body 2 was within the contact section. In one case, this reference system was freely connected to the section, which allowed the section and the origin of the reference system to depart during motion. In the other, the reference system was rigidly connected to body 2 and its origin always coincided with the contact section. The shape functions used with the free attachment were the vibration modes for a free–free rod. Those employed with the rigid attachment were the vibration modes for a clamped–free rod. Fig. 5 depicts both reference systems. The shape functions used

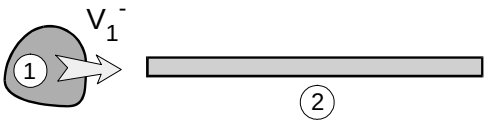

Fig. 3. Axial impact.

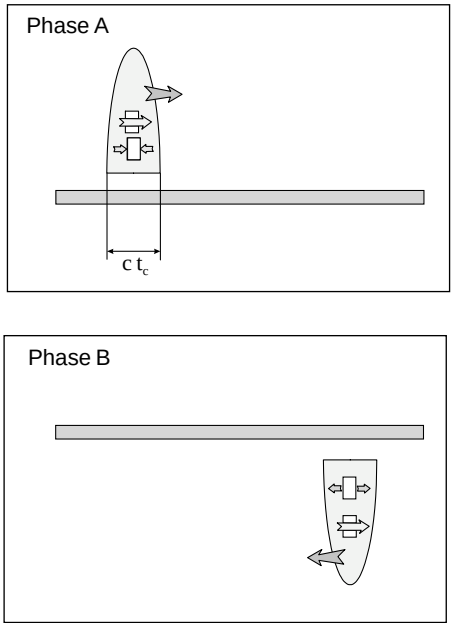

Fig. 4. Wave propagation after axial impact.

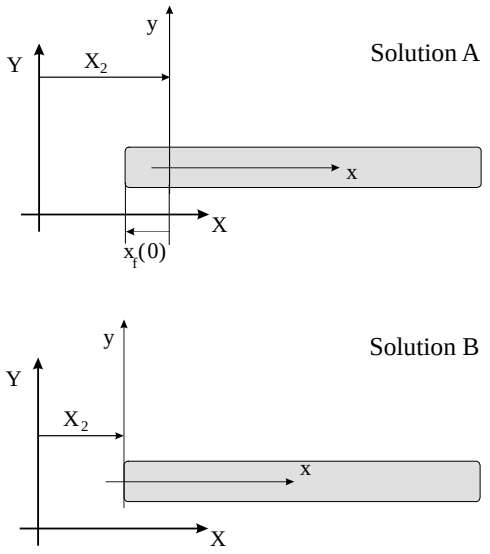

Fig. 5. Reference systems for the flexible beam. Solution A: free attachment, free–free modes; solution B: rigid attachment, clamped–free modes.

were given by the following equations:

$$\begin{aligned} &\textit{Free–free modes}: \quad \varphi_i^f(x) = \cos\left(\frac{i\pi}{L}x\right), \quad i = 1, 2, \ldots, \\ &\textit{Clamped–free modes}: \quad \varphi_i^c(x) = \sin\left(\frac{(2i-1)\pi}{2L}x\right), \quad i = 1, 2, \ldots. \end{aligned} \tag{22}$$

As shown in Ref. [15], the inertial terms were fully uncoupled from the elastic and reference co-ordinates in the case of a free attachment and modes of a free–free rod. On the other hand, the coupling terms for the rigid attachment with a clamped–free rod were non-zero. Based on the form of Eq. (2) in Ref. [15]—this problem required the use of no orientation co-ordinates—the cross-terms of the mass matrix were found to be

$$\begin{aligned} &\textit{Free linkage}: \quad \left(\mathbf{m}_{Rf}\right)_i = \rho A \int_0^L \varphi_i^f(x)\,\mathrm{d}x = 0, \\ &\textit{Rigid linkage}: \quad \left(\mathbf{m}_{Rf}\right)_i = \rho A \int_0^L \varphi_i^c(x)\,\mathrm{d}x = \frac{2m_2}{(2i-1)\pi}. \end{aligned} \tag{23}$$

In order to obtain the contact force from Eq. (20), one must previously calculate the indentation γ between the bodies, which is normally a function of the elastic and reference co-ordinates. In this case, the indentation is given by

$$\gamma = X_1 - \left[X_2 + \sum_i \varphi_i(0) q_{fi}\right], \tag{24}$$

where X_1 is the co-ordinate defining the position of the rigid body 1—which is assumed to be a point—and X_2 is that defining the position of the origin of the reference system attached to the elastic body 2. The procedure used to measure the indentation is illustrated in Fig. 6. Note that,

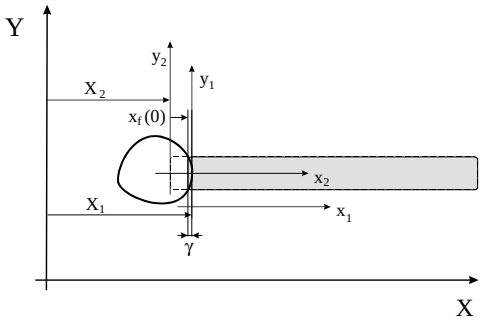

Fig. 6. Indentation during axial impact.

because $\varphi_i^c(0) = 0$ for the clamped–free rod modes, the expression for indentation, and hence the contact force, do not depend on the elastic co-ordinates in the case of the rigid attachment.

Normally, the virtual work of the contact forces is calculated from

$$-F_c\delta\gamma = F_c\left(-\delta X_1 + \left[\delta X_2 + \sum_i \varphi_i(0)\,\delta q_{fi}\right]\right), \tag{25}$$

where

$$F_c = K_h\gamma^{3/2} \quad \text{if } \gamma > 0, \qquad F_c = 0 \quad \text{if } \gamma \leqslant 0. \tag{26}$$

Based on the shape functions used and in Eq. (25), the generalized contact force vector for each type of attachment will be as follows:

$$\textit{Free linkage}: \mathbf{Q}_{Fc} = \begin{bmatrix} -F_c \\ F_c \\ F_c\varphi_1^f(0) \\ \vdots \\ F_c\varphi_n^f(0) \end{bmatrix}, \qquad \textit{Rigid linkage}: \mathbf{Q}_{Fc} = \begin{bmatrix} -F_c \\ F_c \\ 0 \\ \vdots \\ 0 \end{bmatrix}, \tag{27}$$

where vectors are arranged in such a way that the first row corresponds to the co-ordinate of the rigid body 1, the second to the reference co-ordinate of the deformable body 2 and the other n to the elastic co-ordinates of body 2. Note that the generalized contact force vector lacks elastic co-ordinate components in the case of the rigid attachment. Consequently, such co-ordinates can only be excited through the inertial cross-terms (vibration).

The coefficient of restitution is calculated from the definition implicit in Eq. (21). In the example, such a definition reduces to

$$e = -\frac{\left[\mathbf{V}_{RB}^j - \mathbf{V}_{RB}^i\right]^+}{\left[\mathbf{V}_{RB}^j - \mathbf{V}_{RB}^i\right]^-}, \tag{28}$$

where the rigid body velocities are obtained from Eq. (12) in Ref. [15]. Note that the equivalent velocity of the deformable body 2 coincides with $\dot{X}_2$ in the free attachment case but not in the rigid

attachment case, where such a velocity is a linear combination of this variable and the derivatives of the elastic co-ordinates.

Below are discussed the numerical results obtained using the following data: the rigid body had a mass of 0.2 kg and a velocity of 2 m/s prior to colliding. The elastic beam, initially at rest, was assumed to be 1.5 m long and to have a circular cross-section of 1 cm radius, a mass of 4 kg and a modulus of elasticity of 98 GPa. The contact force was calculated on the assumption of a relative curvature of 1.5 cm for the contact surfaces.

By using 30 elastic co-ordinates in the numerical simulations, a final velocity $V_{RB}^{1+} = -1.009\,\mathrm{m/s}$ for the rigid body and $V_{RB}^{2+} = 0.1519\,\mathrm{m/s}$ for the elastic rod were obtained with the free attachment. The corresponding values for the rigid attachment were $V_{RB}^{1+} = -1.018\,\mathrm{m/s}$ and $V_{RB}^{2+} = 0.1524\,\mathrm{m/s}$, respectively. The coefficients of restitution thus calculated were 0.580 for the free attachment and 0.585 for the rigid attachment. With the rigid attachment, the derivative of the reference co-ordinate of the beam—which did not coincide with its rigid body equivalent velocity—upon colliding was $\dot{X}_2^+ = -0.037\,\mathrm{m/s}$. Notice that this value is not even close to the equivalent rigid body velocity of the rod. The coefficient of restitution obtained from this quantity rather than from the rigid body equivalent velocity for the beam was 0.491. This value, which departs from the previous data, lacks physical significance.

Figs. 7 and 8 show the variation of the reference co-ordinates in both simulations. During the first 0.4 ms, co-ordinate X_1 surpassed X_2, so there was some indentation—and hence, contact. Subsequently, the derivative $\dot{X}_2$ was constant with the free attachment but not with the rigid attachment. As noted in Ref. [15], the use of a free attachment and free–free rod vibration modes resulted in the floating system evolving at a constant velocity in the absence of external forces. With the rigid attachment, the origin of the reference system evolved in steps, and so did its attached section. This behaviour is consistent with the wave propagation process depicted in Fig. 4. The velocity derived from Eq. (12) in Ref. [15], which was found to coincide with $\dot{X}_2$ only with a free attachment, remained constant after impact in both simulations.

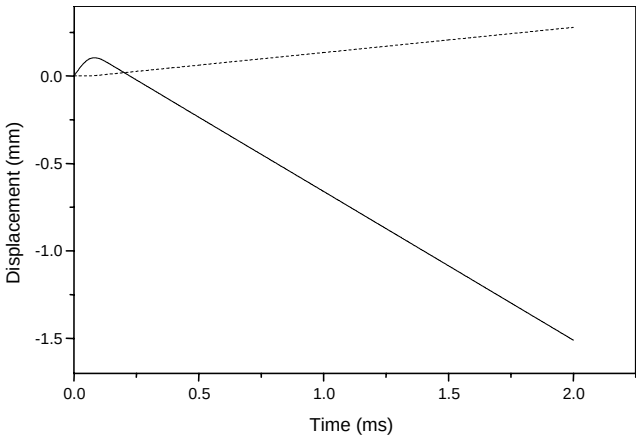

Fig. 7. Variation of the reference co-ordinates with a free attachment: ——, rigid body; ----, flexible rod.

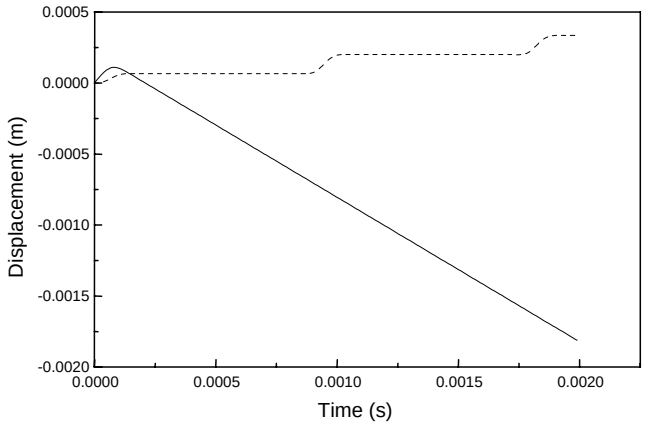

Fig. 8. Variation of the reference co-ordinates with a rigid attachment: ——, rigid body: ----, flexible rod.

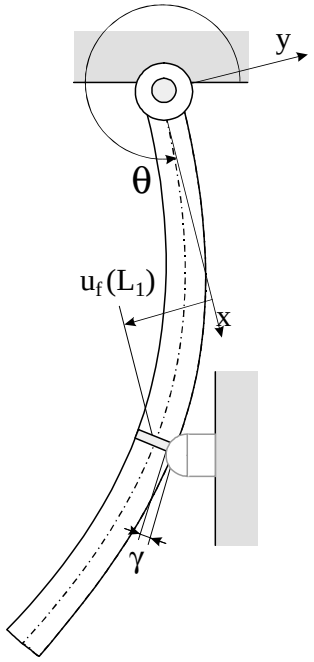

Fig. 9. Transverse impact of a deformable beam.

5.2. *Transverse impact of a flexible pendulum*

This example illustrates the transverse impact of a pin-joined beam on a fixed stop. Fig. 9 shows the deformed pendulum, the elastic displacement undergone by the contact section and the indentation with the fixed stop. Again, the impact was analyzed in two different simulations. In both cases, the origin of the floating reference system was the section of the beam attached to the torque. Both reference systems are shown in Fig. 10. As can be seen, the local x-axis remained tangential to the middle mean fibre of the pendulum in the section attached to the pin joint in the

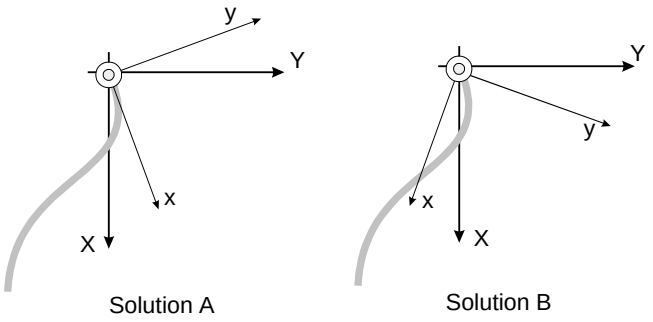

Fig. 10. Floating reference systems for the clamped beam. Solution A: rigid attachment, cantilever modes; solution B: non-rigid attachment, articulated–free modes.

rigid attachment mode but not in the free attachment mode. With this representation, a single reference condition (viz. the angle θ between the local x-axis and the global X-axis) suffices to describe the position of the moving reference system.

The shape functions used to describe the transverse deformation of the beam were the vibration modes for an articulated–free beam with free attachment and those for a cantilever beam with rigid attachment. The corresponding expressions were

$$\phi_i^a(x) = \sin\left(\frac{\mu_i}{L}x\right) + \frac{\sin(\mu_i)}{\sinh(\mu_i)}\sinh\left(\frac{\mu_i}{L}x\right),$$
$$\phi_i^c(x) = \frac{\cosh\left(\frac{\eta_i}{L}x\right) - \cos\left(\frac{\eta_i}{L}x\right)}{\cosh(\eta_i) + \cos(\eta_i)} - \frac{\sinh\left(\frac{\eta_i}{L}x\right) - \sin\left(\frac{\eta_i}{L}x\right)}{\sinh(\eta_i) + \sin(\eta_i)}, \tag{29}$$

where superscripts a and c denote articulated–free and cantilever, respectively. The dimensionless wavenumbers μ_i and η_i are the different roots of the following non-linear equations:

$$\sinh(\mu_i)\cos(\mu_i) = \cosh(\mu_i)\sin(\mu_i),$$
$$\cos(\eta_i)\cosh(\eta_i) = -1. \tag{30}$$

In calculating the vibration modes for the articulated–free beam, both beams were assumed to be subject to no external torque. As a result, the net angular momentum with respect to the clamped end associated to the elastic co-ordinates was always zero. Thus, $\mathbf{m}_{\theta f}$ terms in the mass matrix were all zero with the free attachment but not with the rigid attachment. As shown in Ref. [15], this does not mean that the elastic co-ordinates are uncoupled from the reference co-ordinates in the free attachment since, in addition to the fact that $\mathbf{m}_{\theta\theta}$ depends on the elastic co-ordinates, exist quadratic velocity inertia terms. However, this results in $\omega_{RB} \approx \dot{\theta}$ with the free attachment.

The procedure used to calculate indentation in this impact problem is shown in Fig. 9. This parameter is calculated from

$$\gamma = -L_1 \sin\theta + \cos\theta \sum_i \phi_i(L_1)\, q_{fi}, \tag{31}$$

where L_1 is the distance from the contact point to the beam pin joint. The generalized contact force is given by

$$\mathbf{Q}_{Fc} = F_c \begin{bmatrix} L_1 \cos\theta + \sin\theta \sum_i \phi_i(L_1)\, q_i \\ -\cos\theta \phi_1(L_1) \\ \vdots \\ -\cos\theta \phi_n(L_1) \end{bmatrix}, \quad F_c = K_h \gamma^{3/2}. \tag{32}$$

In this example, the coefficient of restitution is obtained from

$$e = -\frac{[L_1 \boldsymbol{\omega}_{RB}]^+}{[L_1 \boldsymbol{\omega}_{RB}]^-}, \tag{33}$$

where, in general, the rigid body angular velocity will be calculated from Eq. (18) in Ref. [15].

Below are discussed the numerical results obtained using the following data: a pendulum 0.25 m long and the contact point 0.19 m from the clamp. The mass of the beam was assumed to be 0.2 kg and its moment of inertia with respect to the clamp $4.16 \times 10^{-3}\,\mathrm{kg/m^2}$. The beam had a square cross-section of $1.92 \times 10^{-4}\,\mathrm{m^2}$, a moment of inertia of $2.1 \times 10^{-8}\,\mathrm{m^4}$ and a modulus of elasticity of 71 GPa. The relative curvature of the contact surfaces was assumed to be 0.4 m and the angular velocity before impact $\omega_{SR}^- = 10.6\,\mathrm{rad/s}$.

The final rigid body angular velocity of the beam was $\omega_{SR}^+ = -6.286\,\mathrm{rad/s}$ with the free attachment and $\omega_{SR}^+ = -6.302\,\mathrm{rad/s}$ with the rigid attachment. The calculated coefficients of restitution were 0.592 with the free attachment and 0.594 with the rigid attachment. The derivative of the reference angle with the rigid attachment—which did not coincide with the rigid body equivalent angular velocity—immediately after impact was $\dot{\theta}^+ = -75.973\,\mathrm{rad/s}$. Notice the great difference of this value with the beam equivalent rigid body angular velocity. Using this value instead of the rigid body angular equivalent velocity to calculate the coefficient of restitution yielded a value of 7.167, which lacks physical significance and is clearly out of range as it is much greater than unity.

Fig. 11 shows the variation of the reference angle in both simulations and Fig. 12 the derivative of the angle with respect to time. As can be seen, only with the free attachment does the local reference system swings at a—roughly—constant velocity after impact. As noted in Ref. [15], this quantity can vary slightly as a result of the change in the moment of inertia of the beam due to deformation. The angular velocity as defined by Eq. (18) in Ref. [15] remained virtually constant at any time after impact—it only changed beyond the seventh decimal figure.

6. Summary and conclusions

This papers reports a procedure for calculating the kinematic coefficient of restitution for impacts by using numerical simulation. Simulations were done using the *floating frame of reference approach* for deformable bodies. The kinematic coefficient of restitution is the variable to be included in the restitution condition in using rigid body models. In this case, the impact was analyzed via the impulse–momentum balance equations for impulse dynamics, and hence in instantaneous terms. The results obtained in this work apply to bodies that can normally been analyzed as rigid bodies

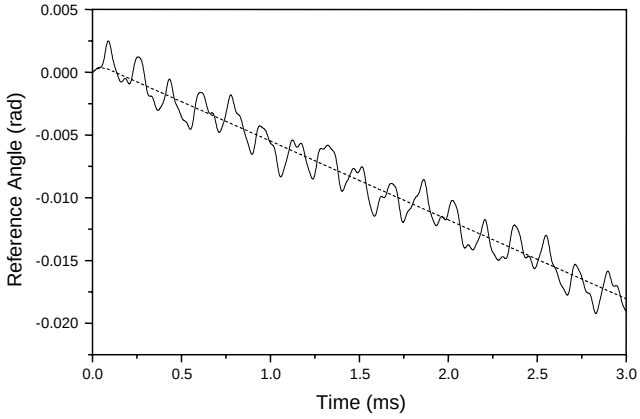

Fig. 11. Reference angle after transverse impact; ----, free attachment, ——, rigid attachment.

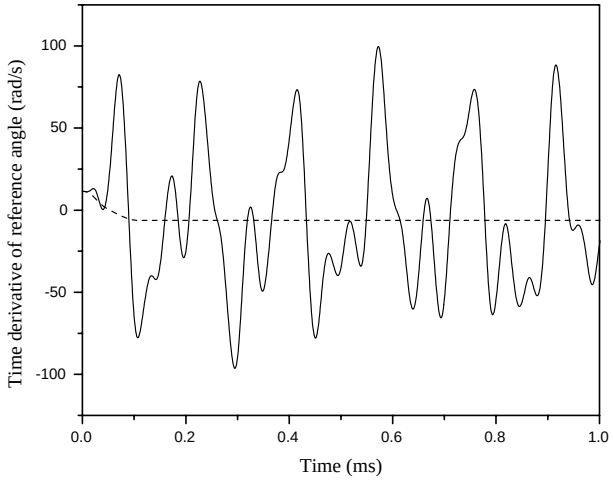

Fig. 12. Reference angular velocities after transverse impact: ----, free attachment; ——, rigid attachment.

except under the conditions of an impact, during which they can absorb a substantial portion of energy in the form of internal vibrations. In this situation, the proposed method for calculating the coefficient of restitution allows impact effects on rigid bodies to be calculated.

For the coefficient of restitution to possess physical significance, the approach and departure velocities at the contact points must be evaluated by excluding deformation terms. This requires the knowledge of the rigid body equivalent velocities acquired by deformable bodies. Such velocities were defined in Ref. [15]. It should be noted that, as a rule, the reference velocities cannot be assimilated to rigid body velocities. Otherwise, the resulting coefficients of restitution obtained lack physical significance as shown in this paper.

Using floating reference systems freely attached to deformable bodies and the vibration models for the free bodies to describe deformation in the bodies provided rigid body equivalent velocities that coincided with the reference velocities. In this case, reference velocities are constant in the

absence of external forces and moments on the bodies. As a rule, the reference velocities do not remain constant after impact when the bodies can move freely in space, as shown by two examples here (one involving an axial impact on a rod and the other a transverse impact of a beam). Based on the results, the coefficients of restitution calculated from an appropriate definition of the approach and departure velocities are consistent with those obtained using different reference conditions and shape functions. If reference velocities are used instead, the resulting coefficients depart substantially from the previous ones as they possess no physical significance.

Acknowledgements

This research was supported, in part, by the Fulbright Foundation and the Spanish Ministry of Science and Technology, under project reference DPI2000-0562.

References

[1] W.J. Stronge, Impact Mechanics, Cambridge University Press, Cambridge, MA, 2000.
[2] W. Goldsmith, Impact, the Theory and Physical Behaviour of Colliding Solids, Edward Arnold, London, 1960.
[3] S. Dubowsky, F. Freudenstein, Dynamic analysis of mechanical systems with clearances Part 1: formation of dynamic model; Part 2: dynamic response, Journal of Engineering for Industry 93 (1) (1971) 305–316.
[4] T.W. Lee, A.C. Wang, On the dynamics of interminent motion mechanisms: Part I. Dynamic model and response, Journal of Mechanisms, Transmissions, and Automation in Design 105 (1983) 534–540.
[5] H.M. Lankarani, P.E. Nikravesh, Continuous contact force models for impact analysis of multibody systems, Nonlinear Dynamics 5 (1994) 193–207.
[6] A.S. Yigit, A.P. Christoforou, Effect of flexibility on low velocity impact response, Journal of Sound and Vibration 217 (3) (1998) 563–578.
[7] J.L. Escalona, Dynamic Analysis of Impacts in Flexible Bars, Ph.D.Thesis, Department of Mechanical Engineering, University of Seville, Spain (in Spanish).
[8] T.J.R. Hughes, R.L. Taylor, J.L. Sackman, A. Curnier, W. Kanoknukulchai, A finite element method for a class of contact–impact problems, Computer Methods in Applied Mechanics and Engineering 8 (1976) 249–276.
[9] S.C. Wu, E.J. Haug, A substructure technique for dynamics of flexible mechanical systems with contact-impact, Journal of Mechanical Design 112 (1990) 390–398.
[10] C.W. Shao, F.W. Liou, A.K. Patra, A contact phase model for the analysis of flexible mechanisms under impact loading, Computers and Structures 49 (4) (1993) 617–623.
[11] H. Palas, W.C. Hsu, A.A. Shabana, On the use of momentum balance and the assumed modes method in transverse impact problems, Journal of Acoustics and Vibration 114 (1992) 364–373.
[12] A.S. Yigit, A.P. Christoforou, Efficacy of the momentum balance method in transverse impact problems, Journal of Vibration and Acoustics 120 (1) (1998) 47–53.
[13] J.L. Escalona, J.M. Mayo, J. Domínguez, A critical study of the use of the generalized impulse–momentum balance equations in flexible multibody systems, Journal of Sound and Vibration 213 (3) (1998) 523–545.
[14] H.M. Lankarani, M.F.O.S. Pereira, Treatment of impact with friction in multibody mechanical systems, in: J.A.C. Ambrosio, W.O. Schiehlen (Eds.), Euromech, Advances in Computational Multibody Dynamics, Lisbon, Portugal, 1999, pp. 129–148.
[15] J.L. Escalona, J. Valverde, J. Mayo, J, Domínguez, Reference motion in deformable bodies under rigid body motion and vibration. Part I: theory, Journal of Sound and Vibration 264 (5) (2003) 1045–1056, this issue.
[16] K.L. Johnson, Contact Mechanics, Cambridge University Press, Cambridge, 1985.
[17] J.L. Escalona, J.M. Mayo, B. Hu, P. Eberhard, Dynamics of axial impacts on rods, Proceedings of the Tenth World Congress on the Theory of Machines and Mechanisms, Oulu, Finland, 1999, pp. 116–121.